Earthquake-Induced Permanent Deformations: Probabilistic Approach

By M. K. Yegian,[1] E. A. Marciano,[2] Members, ASCE, and V. G. Ghahraman,[3] Associate Member, ASCE

Abstract: A simple procedure for estimating earthquake-induced permanent deformations of earth dams, embankments and slopes is presented. The analytical model is based on computed permanent deformations obtained by using Newmark's sliding-block analysis and actual recorded acceleration time histories. The model incorporates the effect of earthquake magnitude through the use of equivalent uniform cycles of motion. Uncertainties in the model and the parameters used are accounted for through the use of modeling error theory. Normalized plots and a computer program are presented that provide the probability that the permanent deformation of a critical sliding mass will exceed a specified value. The results from this probabilistic procedure can be expressed in terms of damage probabilities in the form of a seismic performance analysis matrix. The use of a seismic performance analysis matrix in an overall seismic risk analysis for an earth dam, embankment or a slopes is described in a companion paper.

Introduction

Earthquake-induced permanent deformations of embankments and earth dams can be estimated by a number of approaches of varying degrees of sophistication. On one hand, empirical procedures have been developed to estimate permanent deformations (Ambraseys and Menu 1988; Constantinou and Gazetas 1984; Franklin and Chang 1977; Lin and Whitman 1986; Makdisi and Seed 1978; Newmark 1965; Sarma 1975). On the other hand, two-dimensional finite element methods have been used to evaluate the strain potentials and permanent deformations within a dam subjected to seismic excitations (Chaney 1979; Elgamal et al. 1987; Lee 1974; Paskalov 1984; Prevost et al. 1985; Seed et al. 1975; Serff et al. 1976; Taniguchi et al. 1983). Regardless of the method used, there is always uncertainty in the calculated permanent deformation of an earth dam due to uncertainty in the input parameters and the analysis procedures. In a seismic risk analysis that provides likelihoods of damage or failure of an earth dam, the uncertainty in the predicted response of the dam needs to be considered properly.

In the companion paper (Yegian et al. 1991), the writers describe the use of probabilistic estimates of permanent deformations in the calculation of the overall seismic risk. This paper describes a procedure for calculating earthquake-induced permanent deformations of earth dams and slopes and their likelihood of exceeding. The analytical model developed satisfies the following criteria.

[1]Prof., Dept. of Civ. Engrg., 420 Snell Engrg. Ctr., Northeastern Univ., Boston, MA 02115.

[2]Asst. Prof., Dept. of Civ. Engrg., Northeastern Univ., Boston, MA.

[3]Grad. Student, Dept. of Civ. Engrg., Northeastern Univ., Boston, MA.

Note. Discussion open until June 1, 1991. Separate discussions should be submitted for the individual papers in this symposium. To extend the closing date one month, a written request must be filed with the ASCE Manager of Journals. The manuscript for this paper was submitted for review and possible publication on March 19, 1990. This paper is part of the ***Journal of Geotechnical Engineering***, Vol. 117, No. 1, January, 1991. ©ASCE, ISSN 0733-9410/91/0001-0035/$1.00 + $.15 per page. Paper No. 25414.

1. The seismological and geotechnical parameters used in the model are consistent with output parameters of the seismic hazard analysis described in the companion paper. This allows the incorporation of the model in the seismic risk analysis described in the companion paper.
2. The model parameters can be evaluated using simple or sophisticated procedures as deemed necessary.
3. The permanent deformation model is simple enough to be conveniently applied in design practice, yet it accounts for the pertinent seismic and material parameters.
4. The model allows for the application of probability theory to estimate the likelihood that the permanent deformation will exceed specified values.

Procedure for Calculating Permanent Deformations

Calculation of earthquake-induced permanent deformation can be made using Newmark's sliding block model shown in Fig. 1. In this approach, a rigid-plastic response is assumed, such that every time the acceleration of the block representing a section of an earth dam exceeds a limiting yield level, K_y, then a relative displacement is initiated. The total relative displacement, D_r, represents the permanent deformation of the dam section. An illustration of the motions of the block and the base for a triangular base excitation is presented in Fig. 1. The derived mathematical formulations for D_r, considering triangular, sinusoidal, and rectangular base motions, can be found in Yegian et al. (1988). Based on these derivations for D_r, the following observations are made.

The expression for D_r is of the form

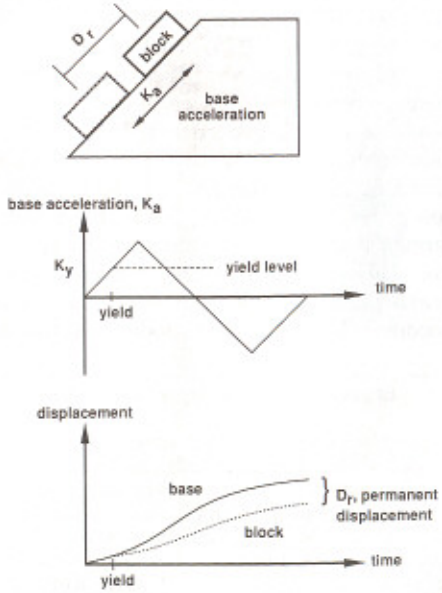

FIG. 1. Sliding Block Analysis for Triangular Base Motion

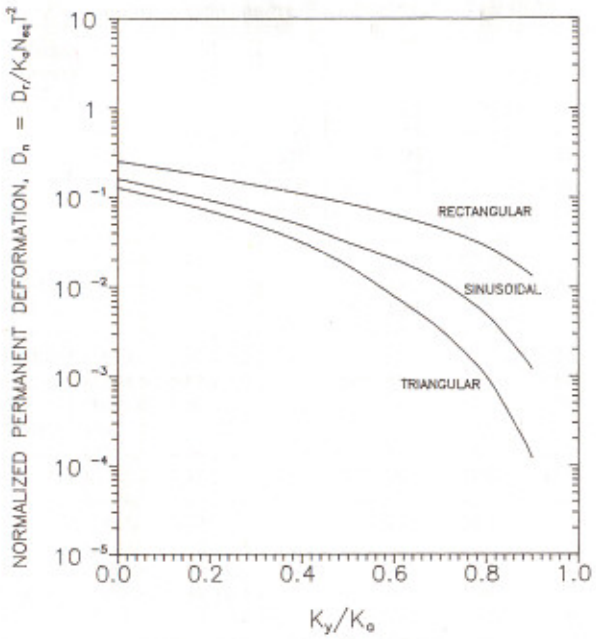

FIG. 2. Normalized Permanent Deformation Functions for Simple Base Motions

$$D_r = f\left(\frac{K_y}{K_a}\right) N_{eq} K_a T^2 \quad \ldots\ldots (1)$$

in which $f(\ )$ = a function that depends on the type of base motion considered; K_y = the yield acceleration; K_a = the peak acceleration of the base; T = the period of the base motion; and N_{eq} = the number of equivalent uniform cycles of base motion. The permanent deformation, D_r, can be normalized with respect to the peak acceleration of the base, K_a, the number of equivalent uniform cycles, N_{eq}, and the square of the period, T, of the base motion, giving

$$D_n = \frac{D_r}{K_a N_{eq} T^2} = f\left(\frac{K_y}{K_a}\right) \quad \ldots\ldots (2)$$

where D_n, referred to as the normalized permanent deformation, is a function of only K_y, K_a, and the type of base motion.

Fig. 2 shows plots of D_n versus K_y/K_a for each of the three simple base motions considered (i.e., triangular, sinusoidal, and rectangular). It is clear that the shape of the base motion has an important effect on the permanent deformation, especially if K_y/K_a is close to 1.0. Recognizing that none of these periodic motions properly simulates the random nature of earthquake-induced ground motions, a more realistic determination of the function $f(\ )$ of Eq. 2 was made by considering actual earthquake records. Franklin and Chang (1977) have published values of permanent deformations computed with Newmark's sliding-block analysis using actual recorded acceleration

TABLE 1. Normalized Permanent Deformation, D_n

Caltech file number (1)	A_g (cm/s^2) (2)	V_g (cm/s) (3)	D_g (cm) (4)	T (s) (5)	N_{eq} (6)	M (7)	R (km) (8)	Normalized Permanent Deformation, D_n: K_y/K_a = 0.02 (9)	K_y/K_a = 0.1 (10)	K_y/K_a = 0.5 (11)
1	341.7	33.40	10.90	0.25	7.30	6.7	9.3	1.03643	0.24957	0.00853
1	210.1	36.90	19.80	0.50	12.37	6.7	9.3	0.29547	0.08894	0.00295
4	175.9	17.70	9.20	0.45	11.72	7.7	43.0	0.26193	0.06840	0.00217
4	152.7	15.70	6.70	0.35	7.64	7.7	43.0	0.65054	0.20652	0.00506
5	128.6	19.30	5.80	0.90	10.25	7.7	89.5	0.11217	0.04076	0.00210
5	87.8	11.80	4.60	0.50	2.55	7.7	89.5	2.22397	0.82716	0.01883
8	252.7	29.40	14.10	0.40	7.28	6.5	24.0	0.35744	0.10213	0.00673
8	164.5	31.60	12.40	0.40	7.23	6.5	24.0	1.07965	0.21470	0.01162
9	155.7	35.60	14.20	0.40	2.50	6.5	40.4	4.69799	1.48476	0.14567
9	197.3	26.00	9.60	0.80	5.28	6.5	40.4	0.20599	0.05761	0.00352
15	81.8	4.90	2.30	0.25	4.74	5.3	11.8	0.32661	0.06127	0.00278
18	175.7	17.10	8.80	0.40	16.74	5.6	40.0	0.12485	0.02767	0.00049
21	130.6	28.70	5.50	0.30	2.92	6.3	47.8	4.55724	0.89018	0.02600
25	142.5	13.30	3.70	0.30	4.79	6.0	6.6	0.40973	0.10308	0.00468
29	274.6	17.00	10.40	0.35	17.93	7.1	16.8	0.21802	0.04754	0.00019
34	425.7	25.40	7.10	0.35	2.57	5.6	32.4	0.48162	0.10156	0.00005
35	269.6	11.80	3.90	0.20	3.04	5.6	34.1	1.22578	0.23570	0.00490
37	340.8	22.50	5.50	0.35	2.50	5.6	31.0	0.30691	0.08023	0.00223
48	250.0	30.00	14.90	0.65	7.89	6.6	22.4	0.36852	0.11676	0.00117
51	122.7	21.90	11.60	0.45	6.40	6.6	42.8	0.90623	0.20338	0.00775
54	147.1	17.40	11.80	0.45	4.80	6.6	41.9	0.76427	0.18729	0.00889
54	117.0	17.30	11.80	0.25	8.54	6.6	41.9	1.89562	0.50925	0.00272
56	309.4	16.50	4.20	0.35	3.35	6.6	28.6	0.33170	0.07531	0.00025
57	103.8	17.00	8.60	0.25	12.76	6.6	37.1	1.51466	0.44697	0.01117
57	148.2	19.40	13.10	0.25	8.13	6.6	37.1	2.05436	0.63395	0.01055
58	167.3	16.50	8.00	0.25	14.40	6.6	37.1	0.55042	0.12347	0.00297
59	133.8	9.60	7.50	0.15	6.56	6.6	39.8	3.58766	0.63993	0.00740
62	130.0	17.60	6.90	0.25	15.03	6.6	42.8	0.96695	0.26725	0.01158
65	146.7	18.00	10.30	0.30	3.55	6.6	40.0	1.57462	0.35048	0.00394
72	82.2	20.80	14.70	0.55	11.48	6.6	39.5	0.46517	0.19484	0.00253
75	133.8	22.30	11.40	0.30	9.92	6.6	40.1	1.38181	0.32545	0.01447
78	126.5	23.20	13.70	0.35	5.54	6.6	42.5	1.90691	0.38457	0.02316
81	198.3	6.20	4.60	0.55	8.29	6.6	32.9	0.04224	0.00528	0.00027
83	158.2	18.30	9.00	0.30	13.50	6.6	40.0	0.53893	0.15179	0.00413
86	104.6	17.40	14.80	0.45	5.47	6.6	49.4	1.64284	0.33307	0.01264
88	209.1	23.50	5.30	0.20	8.37	6.6	34.1	2.23186	0.95016	0.03736
89	139.0	20.70	11.60	0.15	5.12	6.6	44.0	7.48535	1.82801	0.00743
98	236.4	21.80	13.20	0.20	3.34	6.6	42.7	2.98658	0.29061	0.00191
103	120.5	5.40	2.40	0.15	14.56	6.6	45.4	0.79508	0.21155	0.00388
104	103.1	6.00	2.30	0.20	2.34	6.6	52.2	1.39682	0.28464	0.00938
105	83.1	8.30	4.00	0.20	12.04	6.6	38.7	1.50294	0.24775	0.00662
106	188.6	11.60	5.00	0.25	6.04	6.6	36.1	0.43840	0.11578	0.00874
107	107.3	14.30	7.30	0.45	8.36	6.6	39.8	0.57997	0.17608	0.00211
112	78.5	15.70	9.20	0.60	12.18	6.6	40.5	0.30269	0.06277	0.00389
114	110.8	14.00	3.80	0.25	19.04	6.6	32.3	0.82591	0.31662	0.00722
115	220.6	28.20	13.40	0.25	8.76	6.6	29.3	2.24941	0.45679	0.00768
121	119.4	17.10	8.60	0.30	8.39	6.6	41.1	1.47363	0.39242	0.01537
131	184.3	17.20	9.20	0.25	6.23	6.6	38.2	1.17324	0.18555	0.00163
137	129.0	22.30	8.40	0.25	12.63	6.6	29.0	2.31832	0.99565	0.00454
141	145.5	18.00	3.40	0.70	4.10	6.6	29.6	0.29931	0.09356	0.00287
142	143.5	8.60	1.70	0.20	8.47	6.6	26.8	0.46469	0.12316	0.00293

TABLE 1. (*Continued*)

(1)	(2)	(3)	(4)	(5)	(6)	(7)	(8)	(9)	(10)	(11)
143	119.3	4.80	2.00	0.15	7.14	6.6	26.6	0.71666	0.20130	0.00918
144	277.9	12.40	8.90	0.25	9.96	6.6	23.3	0.17475	0.04998	0.00443
145	113.9	31.50	17.50	0.40	16.16	6.6	34.9	1.44375	0.61694	0.02048
148	112.0	17.50	11.10	0.30	15.12	6.6	39.9	0.71143	0.23920	0.00854
166	147.6	15.00	5.40	0.25	8.93	6.6	30.8	0.65921	0.19475	0.01503
176	83.4	20.90	13.70	1.20	13.43	6.6	42.9	0.12738	0.04135	0.00083
185	67.3	4.50	2.10	0.25	18.13	6.6	75.6	0.37238	0.10851	0.00574
186	94.7	9.70	5.00	0.20	13.92	6.6	54.1	1.63655	0.21931	0.00509
187	55.7	3.10	0.70	0.25	11.81	6.6	72.1	0.44795	0.16848	0.00780
188	114.4	17.00	10.80	0.30	6.14	6.6	38.9	1.71738	0.22613	0.00291
192	98.9	19.50	7.90	1.10	12.41	6.6	40.7	0.06154	0.01848	0.00030
198	176.0	20.50	7.28	0.25	5.21	6.6	34.0	1.55839	0.30453	0.01715
217	108.0	14.70	9.94	0.45	8.77	6.6	40.0	0.65739	0.19699	0.00358
221	165.0	6.66	5.91	0.15	9.37	6.6	43.3	0.38380	0.10518	0.00287
223	69.7	4.60	2.07	0.20	6.51	6.6	65.0	1.17383	0.25599	0.00667
233	243.0	31.50	18.30	0.30	14.42	6.6	29.3	0.71493	0.18456	0.00466
233	197.0	17.80	9.46	0.20	13.51	6.6	29.3	1.20139	0.28885	0.00835
236	167.0	13.40	6.13	0.20	8.67	6.6	34.9	1.48072	0.30880	0.00772
239	119.0	17.20	9.79	0.20	16.10	6.6	38.0	1.77936	0.44154	0.01724
239	161.0	19.10	11.60	0.30	4.76	6.6	38.0	2.09633	0.38237	0.01049
241	86.8	17.90	9.22	0.25	20.35	6.6	41.8	1.15174	0.37555	0.01018
241	138.0	19.60	9.98	0.25	3.29	6.6	41.8	4.66397	1.05980	0.03680
244	149.0	18.30	9.80	0.40	2.94	6.6	41.9	1.31834	0.31343	0.01162
246	155.0	16.70	8.29	0.30	7.65	6.6	35.7	1.30254	0.37553	0.00978
251	188.0	18.70	9.49	0.45	3.60	6.6	41.8	0.55156	0.10124	0.00052
253	242.0	19.20	11.40	0.25	3.77	6.6	42.0	1.60448	0.36934	0.00825
255	123.0	22.50	15.80	0.35	11.27	6.6	38.9	1.07231	0.31951	0.00358
261	97.7	18.30	12.20	0.35	11.25	6.6	39.6	1.09191	0.30831	0.00453
262	68.3	25.70	16.50	0.35	11.00	6.6	39.0	2.27025	1.06756	0.03288
262	93.6	27.80	13.70	0.45	5.71	6.6	39.0	1.93945	0.68682	0.02567
265	125.0	18.20	12.60	0.15	8.19	6.6	39.9	4.93423	1.27486	0.01060
266	129.0	21.40	11.60	0.25	10.06	6.6	40.0	1.64744	0.56478	0.00694
267	55.5	13.50	8.49	0.70	11.55	6.6	52.0	0.35384	0.09031	0.00157
267	61.5	13.80	9.38	0.20	8.23	6.6	52.0	7.17646	1.92115	0.00820
312	232.0	11.90	1.66	0.15	2.57	5.8	30.6	1.05718	0.08972	0.00008

time-histories for the base motion. In the research reported herein, 86 of these computed permanent deformations were normalized according to Eq. 2 in order to establish the functional relationship between D_n and K_y/K_a for seismic ground motions.

Table 1 summarizes the normalized deformations D_n for K_y/K_a values of 0.02, 0.1, and 0.5. The peak ground motion parameters and the predominant periods for the records used were obtained from Chang (1978), and their number of equivalent cycles of ground motion from Asturias and Dobry (1982). Fig. 3 shows a plot of these normalized permanent deformations D_n for the three values of K_y/K_a. The determination of the permanent deformation function, $f(K_y/K_a)$, using these data is described in the following section.

Function for Permanent Deformations

To establish the function $f(\ )$ of Eq. 2 based on actual earthquake records, a third-degree polynomial was fitted to the data plotted in Fig. 3, using Lagrange interpolation (Cook 1981). The polynomial was fitted through the

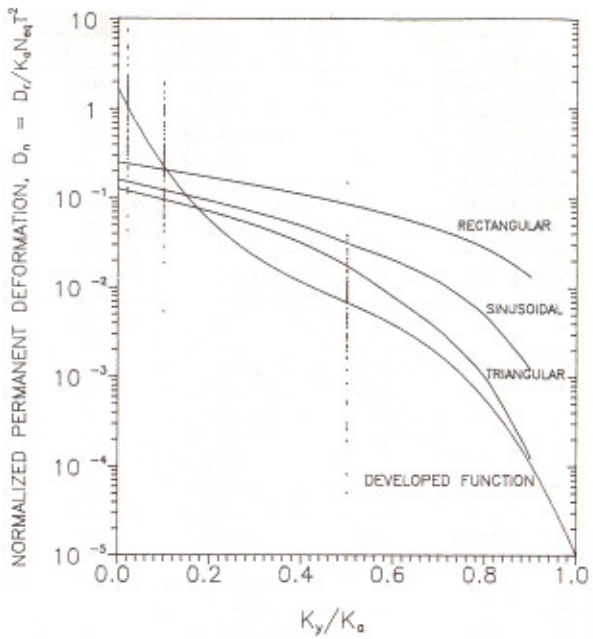

FIG. 3. Normalized Permanent Deformations from 86 Actual Ground Motion Records and Developed Function

median values of the plotted data points at $K_y/K_a = 0.02$, 0.1, and 0.5. The advantage of using the median as opposed to the mean values is that the effect of the few extreme points at the high and low ends, which are orders of magnitude different than the next highest values, is de-emphasized. In addition, D_n was assigned a very small value, 10^{-5}, at $K_y/K_a = 1.0$ because the deformation based on rigid-plastic model should be zero if $K_y/K_a = 1.0$. This value was selected to obtain for $f(K_y/K_a)$, in the range of $0.5 < K_y/K_a < 1.0$ where data are lacking, a shape consistent with that of the triangular base motion. As can be observed in Fig. 3, the triangular base motion appears to be more representative of actual earthquake motion than the sinusoidal or the rectangular base motions. The resulting polynomial curve is shown in Fig. 3, and its mathematical expression is:

$$\log D_n = \log f\left(\frac{K_y}{K_a}\right) = g\left(\frac{K_y}{K_a}\right) = 0.22 - 10.12\left(\frac{K_y}{K_a}\right) + 16.38\left(\frac{K_y}{K_a}\right)^2 - 11.48\left(\frac{K_y}{K_a}\right)^3 \quad \text{..... (3)}$$

Comparison of Developed Function with Other Models

In Fig. 3, the polynomial curve established for the calculation of seismically induced permanent deformations is compared with the deformation functions of the triangular, sinusoidal, and rectangular pulses. For $K_y/K_a <$

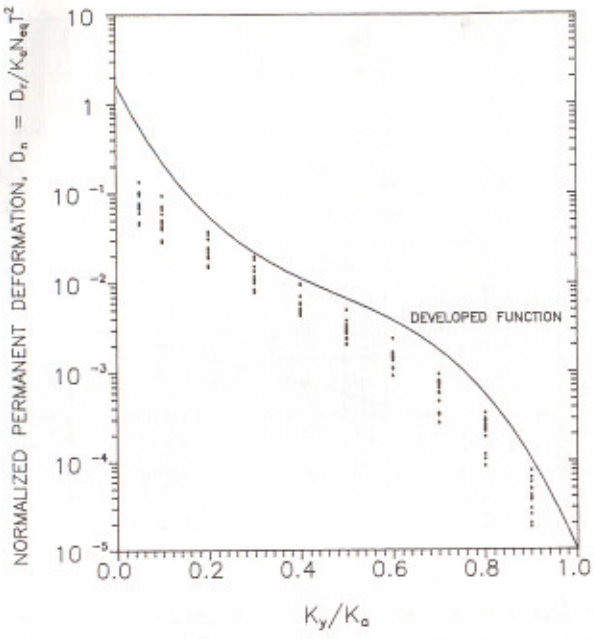

FIG. 4. Comparison of Developed Normalized Permanent Deformation Function with Makdisi and Seed (1978) Data

0.1, these simple base motions yield significantly lower values of D_n than obtained based on the integration of recorded time histories. Conversely, for $K_y/K_a > 0.1$, the sine and the rectangular base motions yield significantly higher values of D_n. For $K_y/K_a > 0.1$, the assumption of a triangular pulse yields deformations that are generally in agreement with data from recorded time histories and thus with the established function for permanent deformations.

Fig. 4 shows values of D_n estimated based on the results of Makdisi and Seed (1978) for magnitudes of 6.5, 7.5, and 8.25. These values of D_n were obtained by normalizing the displacements computed by Makdisi and Seed (1978) with respect to the peak acceleration of the potential sliding mass of the dam, K_a, the square of the first mode fundamental period of the dam, T, and the number of equivalent cycles of the ground motion, N_{eq}. The results obtained plot slightly below the developed function, probably because the periods of the dams used for normalizing Makdisi and Seed (1978) data are larger than the predominant periods of the computed motions of the dam cross sections. Nevertheless, it is noted that data of Makdisi and Seed (1978) plot within the range of data obtained from the integration of recorded time histories.

Uncertainty of Developed Function, $g(K_y/K_a)$

Fig. 3 shows considerable scatter in the values of D_n computed using 86 seismic records for each of $K_y/K_a = 0.02$, 0.1, and 0.5. This observed scat-

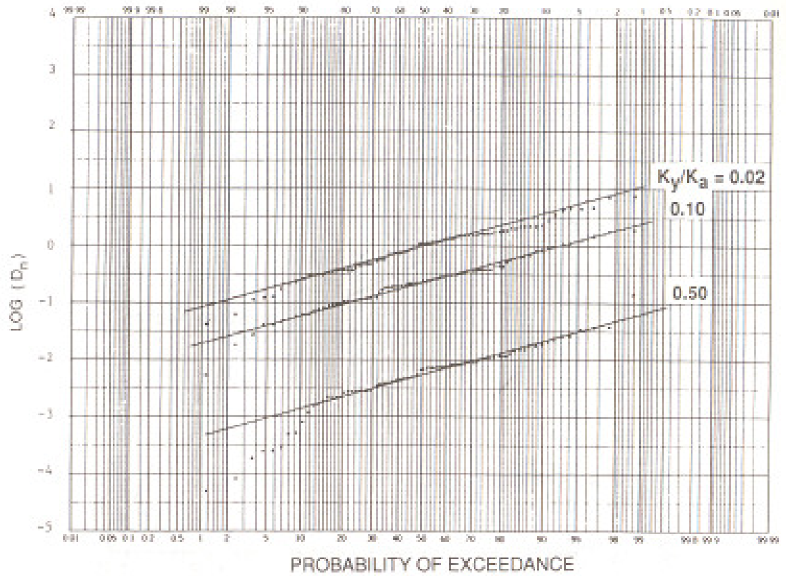

FIG. 5. Probability Plots of Normalized Permanent Deformations from 86 Actual Ground Motion Records for K_y/K_a = 0.02, 0.1, and 0.5

ter of the calculated values of D_n is primarily the result of the inherently random and stochastic nature of seismic ground motions. That is to say, it is not possible to completely define seismic ground motions, and thus their effects, with a finite set of parameters. A similar conclusion was made by Gazetas et al. (1981) when they normalized permanent displacements computed from nine accelerograms recorded during the San Fernando 1971 earthquake. The nine records used were normalized to have common peak acceleration and peak velocity. To account for the resulting uncertainty in the predicted value of D_n given by the function of Eq. 3, statistical analysis of the data shown in Fig. 3 was made. The log D_n values of all the data were plotted on normal probability paper for K_y/K_a = 0.02, 0.1, and 0.5 and are shown in Fig. 5. The results show that for probability of exceeding greater than 10%, D_n is approximately lognormally distributed as is indicated by the nearly log-linear plots of the data on the normal probability paper. These nearly log-linear plots resulted partly because the normalized displacement, D_n, was defined and computed as the product and quotient of several random variables. The slope of each of the three normal probability plots corresponding to the three values of K_y/K_a is about 0.45. Thus, the standard deviation of log D_n, $\sigma_{\log D_n}$, is 0.45. If the values of the parameters K_a, N_{eq}, T, and K_y are known to be exactly equal to specific values, hereafter referred to as k_a, n_{eq}, t, and k_y, then D_n can be simply treated as lognormal with median $\check{d}_n$, where log $\check{d}_n = g(k_y/k_a)$.

The lognormal distribution of D_n was used to calculate contours of probabilities of D_n exceeding specified values d_n. The resulting curves are shown in Fig. 6. An example of the application of Fig. 6 follows. Considering the following parameters: k_a = 0.22g, k_y = 0.07g, n_{eq} = 12 cycles, and t = 0.7

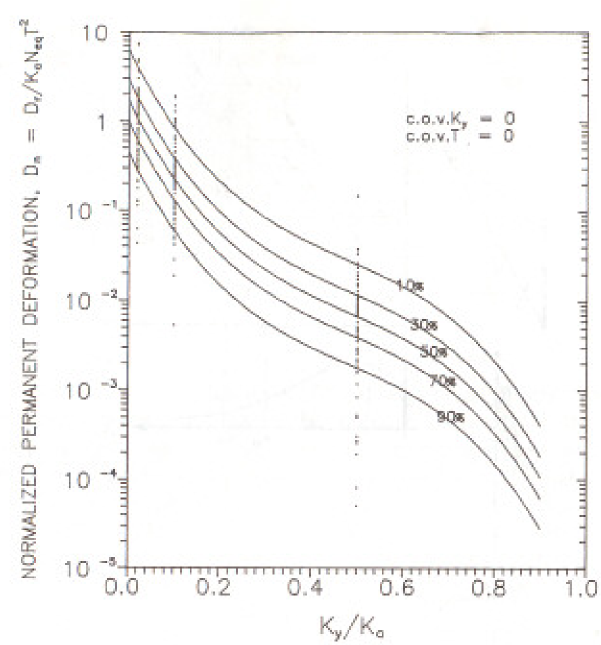

FIG. 6. Probabilities of Exceeding D_n Considering Scatter in Data

s, what is the probability of D_r > 3 ft (0.91 m)? This corresponds to D_n exceeding the following value: $D_n \geq 3/[0.22 \times 32.2 \times 12 \times (0.7)^2]$ = 0.072 for an acceleration ratio: k_y/k_a = 0.07g/0.22g = 0.32. Entering Fig. 6 with these two values yields a probability of about 10% of D_r exceeding 3 ft (0.91 m).

The aforementioned procedure considers the uncertainty in the deformation function introduced by the scatter in the data obtained from the integration of recorded time histories. However, prediction of permanent deformations using the developed function involves additional uncertainties associated with the input parameters K_a, K_y, N_{eq}, and T.

The uncertainty in K_a and N_{eq}, which are treated as ground motion parameters, can be taken into account through the seismic hazard analysis procedure described by the writers in the companion paper (Yegian et al. 1991). The uncertainty in T and K_y must be considered in addition to the uncertainty in the deformation function $g(K_y/K_a)$, in order to make rational calculations of the probability of permanent deformation exceeding a specified level. Using modeling error theory (Ang and Tang 1984), the uncertainty introduced into Eq. 3 by the random nature of seismic ground motions can be represented by

$$\log D_n = g\left(\frac{K_y}{k_a}\right) + S\sigma_{\log D_n} \quad (4)$$

where S = the standard normal variate, which has a mean of zero and standard deviation of 1. Combining Eqs. 2 and 4 yields

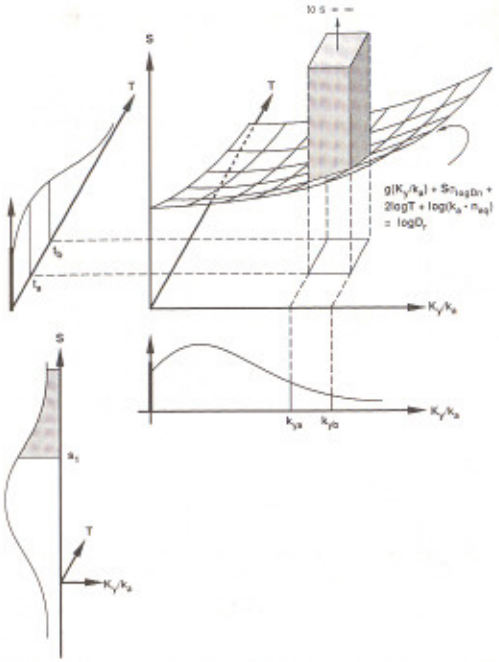

FIG. 7. Schematic Representation of Integrations Shown in Eq. 7

$$\log D_r = g\left(\frac{K_y}{k_a}\right) + S\sigma_{\log D_n} + 2\log T + \log(n_{eq}k_a) \quad \ldots\ldots (5)$$

which defines a surface in a fictitious three-dimensional space above which D_r exceeds a specified value d_r, and below which D_r is less than d_r. The three-dimensional space is illustrated schematically in Fig. 7. The axes are T, K_y/k_a, and S. The procedure for determining the probability of D_r exceeding d_r is to determine the probability that the values of T, K_y/k_a, and S will locate a point lying above the performance surface. To do this, a suitable joint probability distribution is selected for T, K_y, and S, and then it is triple-integrated within the region above the performance surface. The region is defined by $0 \le T \le \infty$, $0 \le k_y \le \infty$, and $s_1 \le s \le \infty$, where

$$s_1 = \frac{\log d_r - \log(k_a n_{eq}) - g\left(\frac{k_y}{k_a}\right) - 2\log t}{\sigma_{\log D_n}} \quad \ldots\ldots (6)$$

The integration is mathematically expressed as

$$P(D_r > d_r | k_a, n_{eq}) = \int_{k_y=0}^{+\infty}\left\{\int_{t=0}^{+\infty}\left[\int_{s=s_1}^{+\infty} f_s(s)ds\right] f_T(t)dt\right\} f_{K_y}(k_y)dk_y \quad \ldots\ldots (7)$$

where $P[D_r > d_r | k_a, n_{eq}]$ = the probability of deformation D_r exceeding a specified value d_r given k_a and n_{eq}; and $f_s(s)$, $f_T(t)$, $f_{K_y}(k_y)$ = the probability

density functions for the random variables, S, T, and K_y, respectively.

The integration was performed numerically in a computer program called NIMPED developed for this purpose (Yegian et al. 1988). The variables T, K_y, and S were assumed to be statistically independent and normally distributed. As the values of T and K_y are necessarily bounded by zero, their distributions were truncated at zero and the probabilities of T and K_y equaling zero were taken to be

$$P(T = 0) = \Phi\left(\frac{-\mu_T}{\sigma_T}\right) \quad \ldots\ldots (8)$$

$$P(K_y = 0) = \Phi\left(\frac{-\mu_{K_y}}{\sigma_{K_y}}\right) \quad \ldots\ldots (9)$$

where μ_T and μ_{K_y} = the means of T and K_y, respectively; and Φ = the cumulative distribution function of the standard normal variate.

The computer program was used to develop typical normalized plots that provide the probabilities of exceeding of any specified deformations, d_r. Figs. 8 and 9 present these plots for *c.o.v.* K_y of 0.5 and 0.2, respectively, and *c.o.v.* T equal to 1/2(*c.o.v.* K_y). Yegian et al. (1988) evaluated the relationship between *c.o.v.* T and *c.o.v.* K_y. The result suggests that, for both cohesionless and cohesive soils, *c.o.v.* T can be considered to be on the order of one-half of *c.o.v.* K_y for a flexible dam on a rigid foundation.

The values of *c.o.v.* K_y that were used to generate the plots were chosen based on values of coefficient of variations of shear strength parameters of cohesionless and cohesive soils, which typically range between 10–15% and 30–50%, respectively (Harr 1977). For cases where there is a potential loss of shear strength due to seismic excitation, *c.o.v.* K_y may be larger than 0.5. In such cases, the computer program NIMPED can be used to get the probabilities of exceeding.

To illustrate the use of this plot, the example presented earlier is considered again but this time with additional uncertainties in K_y and T. Assuming that the coefficients of variation of K_y and T are 0.5 and 0.25, respectively, Fig. 9 can be used to calculate the probability of permanent deformation exceeding 3 ft (0.91 m), $P(D_r > 3$ ft).

The probability contour line, on which the point corresponding to D_n = 0.072 and k_y/k_a = 0.32 plots, defines the probability of deformation exceeding 3 ft (0.91 m). For the example problem, this probability is equal to about 25%. Note that if the uncertainty in K_y and T were not considered, the probability would be about 10%, as was demonstrated earlier and shown by the plots in Fig. 6.

The plots of Figs. 6, 8, and 9 or the program NIMPED can be used to determine the complementary cumulative distribution curve for D_r, conditioned upon specified values of k_a and n_{eq}. In Fig. 10 the curve corresponding to *c.o.v.* K_y = 0.5 shows the resulting distribution for the example. This curve can be used to determine the probabilities of the occurrence of different damage states. For example, if a permanent deformation greater than 3 ft (0.91 m) is considered catastrophic because of potential overtopping of a dam, and if deformation of less than 1 ft (0.305 m) is considered inconsequential, then the following damage states with their corresponding probabilities can be defined from Fig. 10 (*c.o.v.* K_y = 0.5): $P(O) = P$(minor or no) = $P[D_r < 1$ ft (0.305 m)] = 0.57; $P(H) = P$(heavy) = P[1 ft (0.305

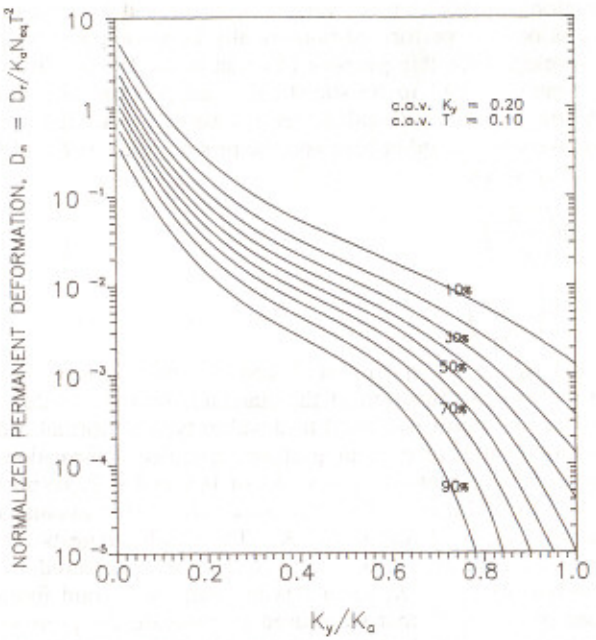

FIG. 8. Probability Contours of Normalized Permanent Deformation

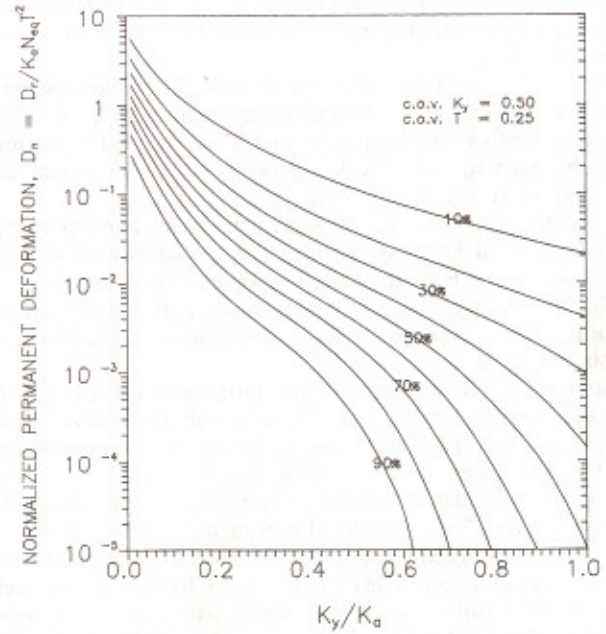

FIG. 9. Probability Contours of Normalized Permanent Deformation

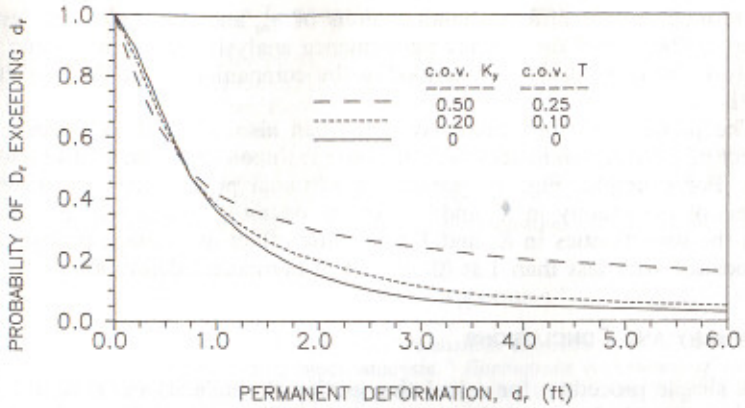

FIG. 10. Complementary Cumulative Distributions of Permanent Deformation for the Example (1 ft = 0.305 m)

m) $\geq D_r < 3$ ft (0.91 m)] = 0.18; and $P(C) = P$(catastrophic) $= P[D_r \geq 3$ ft (0.91 m)] = 0.25. The results of this probabilistic permanent deformation analysis can be conveniently displayed in a damage probability matrix. Table 2 shows a typical seismic performance analysis matrix involving probability of exceedance of earthquake-induced permanent deformation. The damage probabilities obtained from the aforementioned example are displayed as a single column in this matrix, for the peak ground acceleration, A, in the range $0.15g \leq A < 0.2g$, which corresponds to $k_a = 0.22g$. In order to perform an overall seismic risk analysis, these computations need

TABLE 2. Typical Damage Probability Matrix from Permanent Deformation Analysis

Damage state (1)	Number of Equivalent Cycles 1–5 (2)	5–10 (3)	10–15 (4)	15–20 (5)	20–25 (6)
(a) $0.0g \leq A < 0.15g$					
No/minor (O), < 1 ft	—	—	—	—	—
Heavy (H), 1–3 ft	—	—	—	—	—
Catastrophic (C), > 3 ft	—	—	—	—	—
(b) $0.15g \leq A < 0.2g$					
No/minor (O), < 1 ft	—	—	0.57	—	—
Heavy (H), 1–3 ft	—	—	0.18	—	—
Catastrophic (C), > 3 ft	—	—	0.25	—	—
(c) $A \geq 0.20g$					
No/minor (O), < 1 ft	—	—	—	—	—
Heavy (H), 1–3 ft	—	—	—	—	—
Catastrophic (C), > 3 ft	—	—	—	—	—

Note: 1 ft = 0.305 m.

to be repeated for different combinations of n_{eq} and A to fill in the entire matrix. The use of the seismic performance analysis matrix in seismic risk analysis for earth dams is described in the companion paper (Yegian et al. 1991).

The probabilistic procedure presented can also be used to evaluate the effect of critical parameters and uncertainties upon the estimated probabilities. For example, Fig. 10 presents conditional probabilities for different levels of uncertainty in K_y and T. For the example considered, it is noted that the uncertainties in K_y and T have little effect on damage probabilities associated with less than 1 ft (0.305 m) of permanent deformation.

Summary and Conclusions

A simple procedure for calculating earthquake-induced permanent deformation of earth dams and slopes is presented. The analytical model can provide estimates of the probability of the permanent deformation of a dam exceeding a specified value given a specified seismic event characterized by the average acceleration and the number of uniform cycles of motion of a critical sliding mass. A computer program, NIMPED, is available that facilitates the probability calculations. Using this program, charts of exceeding probabilities of permanent deformation are provided considering typical levels of uncertainty in input parameters. These charts or the computer program can be used to develop damage probability matrices for an earth dam. The results from such a seismic performance analysis can be used in an overall seismic risk analysis of an earth dam, as described in the companion paper (Yegian et al. 1991). In addition, the probabilistic procedure presented can help identify the important parameters and uncertainties that require special considerations in the evaluation of permanent deformation.

The model developed for calculating permanent deformation is based on the assumption that the soil deforms as a rigid-plastic mass. Also the predominant periods of most of the records used are less than 0.5 s. Improvements in the model can be made by considering elastoplastic soil response and earthquake records with larger periods associated with soil deposits.

Acknowledgments

The research described in this report was sponsored by the National Science Foundation through Grant No. DFR-84-12124 for research on Integrated Seismic Risk Analysis for Earth Dams. The writers gratefully acknowledge this support.

Appendix I. References

Ambraseys, N. N., and Menu, J. M. (1988). "Earthquake-induced ground displacements." *Earthquake Engrg. and Struct. Dynamics*, 16, 985–1006.
Ang, A., and Tang, W. H. (1984). *Probability concepts in engineering planning and design*. Vol. II, John Wiley and Sons, New York, N.Y.
Asturias, R. W., and Dobry, R. (1982). "The equivalent number of cycles of recorded accelerograms for soil liquefaction studies." *Report No. CE-82-5*, Rensselaer Polytech. Inst., Troy, N.Y.
Chaney, R. C. (1979). "Earthquake induced deformations in earth dams." *Proc. Second U.S. Nat. Conf. on Earthquake Engrg.*, Earthquake Engrg. Res. Inst., 633–642.
Chang, F. K. (1978). "Catalogue of strong motion earthquake records, Volume I, Western United States, 1933–1971." *State-of-the-Art for Assessing Earthquake Hazards in the United States*, Rept. 9, Misc. Paper No. S-73-1, U.S. Army Engr. Waterways Experiment Station, Vicksburg, Miss.
Constantinou, M., and Gazetas, G. (1984). "Probabilistic seismic sliding deformations of earth dams and slopes." *Proc. Fourth ASCE Specialty Conf. on Probabilistic Mech. and Struct. Reliability*, ASCE, 318–321.
Cook, R. D. (1981). *Concepts and applications of finite element analysis*. John Wiley and Sons, New York, N.Y.
Elgamal, A. W., Abdel-Ghaffar, A. M., and Prevost, J. H. (1987). "2-D elastoplastic seismic shear response of earth dams: Application." *J. Geotech. Engrg. Div.*, ASCE, 113(5), 702–719.
Franklin, A. G., and Chang, F. K. (1977). "Permanent displacements of earth embankments by Newmark sliding block analysis." *Earthquake Resistance of Earth and Rock-Fill Dams*, Rept. 5, Misc. Paper No. S-71-17, U.S. Army Engr. Waterways Experiment Station, Vicksburg, Miss.
Gazetas, G., DebChaudhury, A., and Gasparini, D. A. (1981). "Random vibration analysis for the seismic response of earth dams." *Geotechnique*, 31(2), 267–277.
Harr, M. (1977). *Mechanics of particulate media*. McGraw-Hill, New York, N.Y.
Lee, K. L. (1974). "Seismic permanent deformations in earth dams." *Rept. No. UCLA-ENG-7497*, U.C.L.A., Los Angeles, Calif.
Lin, J. S., and Whitman, R. V. (1986). "Earthquake induced displacements of sliding blocks." *J. Geotech. Engrg. Div.*, ASCE, 112(1), 44–59.
Makdisi, F. I., and Seed, H. B. (1978). "Simplified procedure for estimating dam and embankment earthquake-induced deformations." *J. Geotech. Engrg. Div.*, ASCE, 104(7), 849–867.
Newmark, N. M. (1965). "Effects of earthquakes on dams and embankments." *Geotechnique*, 15(2), 139–160.
Paskalov, T. A. (1984). "Permanent displacement estimation on embankment dams due to earthquake excitations." *Proc. 8th World Conf. on Earthquake Engrg.*, Earthquake Engrg. Res. Inst., 327–334.
Prevost, J. H., Abdel-Ghaffar, A. M., and Lacy, S. J. (1985). "Nonlinear dynamic analysis of an earth dam." *J. Geotech. Engrg. Div.*, ASCE, 111(7), 882–897.
Sarma, S. K. (1975). "Seismic stability of earth dams and embankments." *Geotechnique*, 25(4), 743–761.
Seed, H. B., Lee, K. L., Idriss, I. M., and Makdisi, F. I. (1975). "The slides in the San Fernando dams during the earthquake of February 9, 1971." *J. Geotech. Engrg. Div.*, ASCE, 101(7), 651–688.
Serff, N., Seed, H. B., Makdisi, F. I., and Chang, C. Y. (1976). "Earthquake induced deformation of earth dams." *Report No. EERC 76-4*, Univ. of California, Berkeley, Calif.
Taniguchi, E., Whitman, R. V., and Marr, W. A. (1983). "Prediction of earthquake-induced deformation of earth dams." *Soils and Found.*, 23(4), 126–132.
Yegian, M. K., Marciano, E. A., and Ghahraman, V. G. (1988). "Integrated seismic risk analysis for earth dams." *Report No. 88-15*, Northeastern Univ., Boston, Mass.
Yegian, M. K., Marciano, E. A., and Ghahraman, V. G. (1991). "Seismic risk analysis for earth dams." *J. Geotech. Engrg.*, ASCE, 117(1), 18–34.

Appendix II. Notation

The following symbols are used in this paper:

A = peak ground acceleration;
$c.o.v.\ K_y$ = coefficient of variation of K_y;
$c.o.v.\ T$ = coefficient of variation of T;
D_n = normalized permanent deformation;

D_r = permanent deformation;
$\hat{d}_n$ = median value of normalized permanent deformation;
d_r = specified permanent deformation;
$f_T(t)$ = probability distribution function of T;
g = gravitational constant;
K_a = average acceleration of a critical sliding mass;
K_y = yield acceleration of a critical sliding mass;
N_{eq} = number of equivalent uniform cycles;
S = standard normal variate;
T = period of motion of a critical sliding mass;
μ_{K_y} = mean value of K_y;
μ_T = mean value of T;
$\sigma_{\log D_n}$ = standard deviation of log D_n; and
Φ = cumulative distribution function for the standard normal variate.